The Birefringence Problem in Optical Disk Substrates: A Modeling Approach

An analytical model has been constructed to predict the birefringence level in an injuection-molded disk with direct application to optical disk substrates. The model incorporates simplified analyses for the flow in a center-gated cavity during the filling stage, the heat transfer during the cooling stage, and the stress relaxation following the cessation of flow at the end of the filling stage of the injection-molding cycle. The stress relaxation process is analyzed with the integral constitutive equation of Wagner and the residual stresses are converted to retardation via the stress-optical law. Predictions of normal retardation profiles are in line with experimental data and the general effects of melt temperature, mold temperature, and injection speed are closely captured by the model. By contrast, the observed transverse retardation is not in accord with the predicted response. This discrepancy is attributed to the fact that the transverse retardation is induced by cooling stresses and thus cannot be explained in terms of a flow stress mechanism employed in the present analysis.

Jehuda Greener
Raymond Kesel
Beverly A. Contestable
Diversified Technologies Group Research Laboratory
Eastman Kodak Company
Rochester, NY 14650

Introduction

Optical data storage is emerging as a key technology in the computer and information systems of the coming decade. Extremely high storage density, very compact drives, and the absence of physical contact between heads and media are among the main advantages of this technology over competing technologies such as magnetics. The use of plastic substrates in optical memory disks has enabled this technology to make strong inroads into the high-volume consumer markets, as exemplified by the commercial and technological success of the audio compact disk and the laser videodisk (e.g., Kirkland, 1986; Kaempf et al., 1987).

In light of this success many new optical storage systems have been designed around a rigid plastic substrate. A schematic structure of an optical disk with a plastic substrate is shown in Figure 1. In this so-called "substrate-incident" configuration the substrate is positioned between the optical head and the storage medium and its main function, other than supporting the medium, is to protect it from dust and abrasion. In general, in order to achieve high recording performance the substrate must be produced to extremely tight tolerances and it must possess outstanding dimensional stability, high transmittance, and low optical anisotropy (birefringence).

The minimization of birefringence is especially critical in the case of magneto-optical systems where the storage mechanism is based on the Kerr effect (see Yoshizawa and Matsubayashi, 1986; Marchant, 1986a; Ojima et al., 1986). In these systems retardation levels in excess of 20–30 nm (double pass) may have a detrimental effect on the carrier-to-noise ratio and other performance measures of the storage device. In general, low birefringence can be attained either through use of materials with low intrinsic optical anisotropy or through judicious manipulation of the injection-molding process—the most widely used process for producing plastic substrates (Kirkland, 1986). To date, the latter option appears to be more viable since very few materials with low intrinsic anisotropy that are suitable for optical disk applications have so far been developed on a commercial scale (Kato et al., 1986; Kaempf et al., 1987). However, since injection molding is a strongly "orienting" process, attainment of low birefringence may be a particularly daunting task, requiring careful selection and balancing of the key molding conditions.

In this study we present an analytical model to predict the birefringence (orientation) buildup during the injection-molding process with direct application to optical disk substrates. Although the general mechanisms for the development of molecular orientation in injection molding have been recognized for some time (Spencer and Gilmore, 1951; Ballman and Toor, 1960; Isayev and Crouthamel, 1984), only a few attempts have

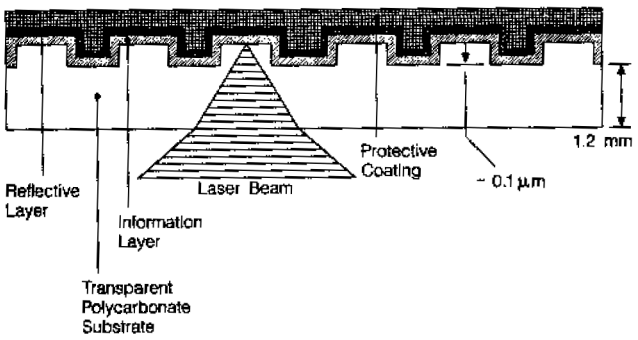

Figure 1. Cross section of an optical storage disk.

been made to describe the associated phenomena by quantitative physical models. The first such attempt was made by Dietz, White, and Clark (1978), who developed a simplified algorithm to predict the birefringence distribution in a molded slab using a linear viscoelastic model with limited utility in real molding problems. This general algorithm was later improved upon in two separate studies, one by Isayev and Hieber (1980; see also Isayev, 1983) and the other by Greener and Pearson (1983). In both studies the linear constitutive model was replaced with nonlinear rate models (Leonov's and Marrucci's respectively) and generally good agreement with experimental data was demonstrated. The model in the present work is based on an algorithm similar to those used in the latter studies but it differs in two respects:

1. The model is adapted to tackle the particular geometry of a substrate mold cavity, namely, that of a center-gated disk.

2. More importantly, the constitutive equation used in the present formulation is a nonlinear integral model of the factorized Rivlin-Sawyers type (Bird et al., 1987) first proposed by Wagner (Wagner, 1976, 1979; Wagner and Stephenson, 1979). Despite some fundamental deficiencies (Larson and Monroe, 1984), this constitutive equation is chosen over other nonlinear models owing to its relative simplicity, versatility, and its proven ability to describe quantitatively the dynamics of viscoelastic liquids in a wide range of transient flows (see, for example, Wagner et al., 1979; Menezes, 1980; Greener and Connelly, 1986), which is of particular importance in modeling the problem in question.

Model Formulation

In a typical process cycle the molten polymer is injected into a cold mold through a long and slightly tapered sprue. It enters into the cavity through a circular (rim) gate and then spreads radially until the cavity fills. Depending on the dimensions of the cavity, fill times may range from 0.1 to 1.0 s. The flow geometry is depicted schematically in Figure 2. The corresponding radial flow problem has been studied extensively in the literature (Lawrencena and Williams, 1974; Middleman, 1976; Co, 1981; Goyal et al., 1988) and is fairly well understood both for the Newtonian and non-Newtonian cases. The velocity field of this flow is given by

$$u_r = \frac{a(z,t)}{r}, \quad u_z = u_\phi = 0 \tag{1}$$

where a is a model-dependent function of z and time. The rate-

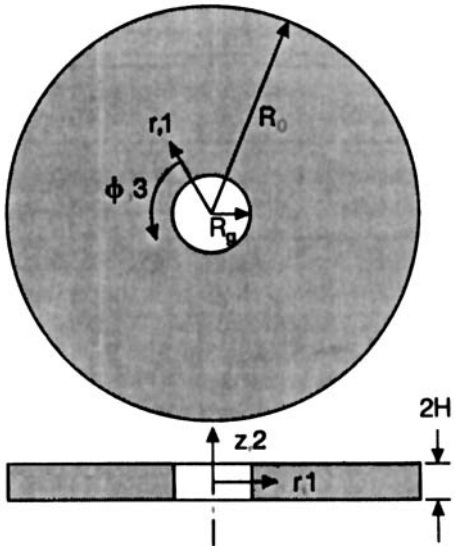

Figure 2. Geometry of a center-gated disk.

of-strain tensor for this flow can be easily derived to give:

$$\dot{\gamma} = \begin{pmatrix} -2\frac{a}{r^2} & \frac{a'}{r} & 0 \\ \frac{a'}{r} & 0 & 0 \\ 0 & 0 & 2\frac{a}{r^2} \end{pmatrix} \tag{2}$$

where $a' \equiv da/dz$. Thus, kinematically radial flows are mixed flows since $\dot{\gamma}$ contains both shear and extensional components. It can be shown, however, that the extensional components decay with r and the flow becomes shear-dominated a short distance from the center of the disk. The shear rate for this flow is given by

$$\dot{\gamma} = \sqrt{\frac{1}{2}\Pi_{\dot{\gamma}}} = \sqrt{\left(\frac{a'}{r}\right)^2 + 4\frac{a^2}{r^4}} \tag{3}$$

The dashed-underlined term decays rapidly with r and is usually negligible over a typical "information" range on the optical disk. (In typical data storage disks the "information" range starts at a radial distance r/H of ~40.) In order to evaluate the shear rate in the cavity $a(z)$ must be specified. For the special case of a power-law fluid (Middleman, 1976),

$$a = \frac{Q}{4\pi H^{q+1}}\left(\frac{q+1}{q}\right)(H^q - z^q) \tag{4}$$

where $q = 1 + 1/n$, n is the power-law index, and Q, the volumetric flow rate, is simply related to the fill time by

$$Q = \frac{2\pi H(R_o^2 - R_g^2)}{t_{\text{fill}}} \tag{5}$$

In order to approximately account for the nonisothermal conditions in the cavity during the filling stage, we consider the presence of a "skin," i.e., the frozen layer that builds up on the cavity walls during flow due to the cooling near the mold surfaces. The existence of a structurally distinct skin layer has been inferred from birefringence data (e.g., Wales et al., 1972) and it has been analyzed to varying degrees of rigor by Dietz et al. (1978), Janeschitz-Kriegl (1977, 1979), Richardson (1983) and Kamal et al. (1988). In the present analysis we follow the approximate approach of Dietz et al. to estimate the skin layer thickness

$$\delta \simeq 1.9 \frac{T_g - T_{\text{mold}}}{T_{\text{melt}} - T_{\text{mold}}} \sqrt{\beta t_c} \tag{6}$$

where β is the thermal diffusivity and t_c, the contact time, is given by

$$t_c = t_{\text{fill}} \frac{R_o^2 - r^2}{R_o^2 - R_g^2} \tag{7}$$

Although δ is a function of r, it is assumed that $\partial\delta/\partial r$ is sufficiently small that the one-dimensional character of the flow is preserved. Also, we assume that the flow in the core is isothermal and steady and that the polymer melt obeys the power law. With these assumptions, Eq. 3 can be simply modified by replacing H with $H_{\text{eff}} \equiv H - \delta$ and, together with Eq. 4, it can be used to evaluate the shear rate distribution in the cavity at the instant of fill. For the stated assumptions the pressure drop in the cavity can be estimated from

$$\Delta P = K \left[\frac{(q+1)Q}{4\pi}\right]^n \int_{R_g}^{R_o} \frac{dr}{r^n H_{\text{eff}}^{2n+1}} \tag{8}$$

where K is the consistency index in the power-law model and H_{eff} $(= H - \delta)$ is the effective half depth of the radial flow space. This pressure is the filling pressure, i.e., the minimum pressure needed to completely fill the cavity at the given rate.

With the kinematics completely specified, it is now possible to estimate the hydrodynamic stresses at the instant of fill (and thereafter) via an appropriate constitutive model. The model selected is an integral equation of the Rivlin-Sawyers type first proposed by Wagner (Wagner, 1976, 1979; Wagner and Stephenson, 1979). In its simplest form Wagner's equation can be written as

$$\tau = \int_{-\infty}^{t} \mu(t - t') \cdot h[\mathrm{I}_c(t, t'), \mathrm{II}_c(t, t')] \cdot \boldsymbol{C}^{-1}(t, t')\, dt' \tag{9}$$

where τ is the extra stress, $\boldsymbol{C}^{-1}$ is the Finger strain tensor and I_C and II_C are its first and second invariants. Here μ and h are the time-dependent and strain-dependent components of the memory function; μ can be expressed by a sum of exponentials,

$$\mu(t - t') \equiv \mu(s) = \sum_{i=1}^{m} \mu_i \exp\left(-\frac{s}{\lambda_i}\right) \tag{10}$$

where μ_i and λ_i are characteristic constants that can be extracted from linear viscoelastic data. For shear-dominated flows, the strain-dependent (damping) function can be written as

$$h = \exp\left[-b(\mathrm{I}_c - 3)^{1/2}\right] \tag{11}$$

where b is the only "nonlinear" parameter in the Wagner model. Also, for shear flows we have

$$\mathrm{I}_c = \mathrm{II}_c = [\gamma(t, t')]^2 + 3 \tag{12}$$

where $\gamma(t, t')$ $[\equiv \gamma(t) - \gamma(t')]$ is the relative shear strain and

$$\gamma(t) = \int_0^t \dot{\gamma}(t'')\, dt'' \tag{13}$$

If we assume a steady state during the filling stage, Eq. 9 together with Eqs. 3 and 4 can be used to calculate the stress distribution in the cavity at the instant of fill. As soon as the cavity fills, flow effectively ceases and the stresses in the cavity start to decay (relax) rapidly. Since the filling stage is typified by relatively high shear rates, the relaxation process is expected to be nonlinear in the rheological sense, i.e., the normalized relaxation function is expected to depend on the absolute level of the initial stress at any given position. The temporal change in shear stress τ_{12} and the first normal stress difference N_1 following the cessation of a steady shear flow can be derived from Eq. 9 to give (Menezes, 1980)

$$\tau_{12}(t) = \dot{\gamma} \int_t^{\infty} G(s) \frac{\partial}{\partial s} \{(s - t)\, h[\dot{\gamma}(s - t)]\}\, ds \tag{14}$$

and

$$N_1(t) = \dot{\gamma}^2 \int_t^{\infty} G(s) \frac{\partial}{\partial s} \{(s - t)^2\, h[\dot{\gamma}(s - t)]\}\, ds \tag{15}$$

where

$$G(s) = \int_s^{\infty} \mu(s')\, ds'$$

is the relaxation shear modulus of linear viscoelasticity. Since the material in the cavity is cooling rapidly, concurrent with the stress relaxation process, Eqs. 14 and 15 must be modified to account for the changes in temperature. We treat this nonisothermal problem using the general approach of Matsui and Bogue (1977), which is readily adaptable to the Wagner equation. Their formulation weighs the relaxation times by the local temperature histories based on Boltzmann's superposition principle, and essentially modifies the temperature-dependent component of the memory function μ leaving the damping function h intact. The nonisothermal version of Wagner's equation then takes the form

$$\tau = \sum_i g_i^0 \frac{T(t)}{T_0} \int_{-\infty}^{t} \frac{\exp\left[-\int_{t'}^{t} \frac{dt''}{\lambda_i(t'')}\right]}{\lambda_i(t')} \cdot h(\mathrm{II}_c)\, \boldsymbol{C}^{-1}(t, t')\, dt' \tag{16}$$

where T_0 is a reference temperature, $\lambda_i(t'') = \lambda_i(T_0) \cdot a_T[T(t'')]$, and $g_i^0 = \mu_i \lambda_i(T_0)$. The term a_T is the time-temperature shift factor that expresses the temperature dependence of the relaxation time (or the zero-shear viscosity) of the material. We use two expressions for a_T, one, a WLF type, for temperatures in the range $T_g < T < T_g + 100°\text{C}$,

$$\log a_T = -\frac{C_1(T - T_0)}{C_2 + T - T_0} \tag{17}$$

and a second, an Arrhenius type, for $T > T_g + 100°C$,

$$a_T = A \exp\left(\frac{B}{T}\right) \tag{18}$$

C_1, C_2, A and B are material constants. These general expressions for a_T are consistent with established behavior of polymer melts (Ferry, 1970).

To complete this analysis it is necessary to specify the temperature distribution and its evolution during the cooling stage. We use the result for the one-dimensional heat conduction problem with isothermal boundaries (Bird et al., 1960),

$$\frac{T - T_{\text{mold}}}{T_{\text{melt}} - T_{\text{mold}}} = 2 \sum_{m=0}^{\infty} \frac{(-1)^m}{(m + 1/2)\pi} \cdot \exp\left[-(m + 1/2)^2 \pi^2 \beta t / H^2\right] \cos\left[(m + 1/2)\frac{\pi z}{H}\right] \tag{19}$$

where T_{mold} is the surface temperature in the cavity, T_{melt} is the average temperature of the melt when injected into the cavity, and β, the thermal diffusivity, is assumed constant. Equation 19 is a valid approximation throughout the cavity space except for the edges where the heat transfer is two-dimensional. The stresses in the cavity will continue to relax so long as the material is molten, i.e., $T > T_g$. As soon as the material vitrifies, the relaxation process becomes exceedingly slow (the relaxation time is effectively infinite) and, ultimately, the unrelaxed stresses "freeze" in the solid matrix. As pointed out in previous studies (Isayev and Crouthamel, 1984; Greener and Pearson, 1983), these stresses are the chief contributor to the state of orientation and anisotropy in the molded article. Other sources of orientation will be discussed in the Results Section.

The stress-optical law is now invoked to convert the residual stresses to birefringence. This law states that the birefringence and the principal stress difference are proportional,

$$\Delta n = C \cdot \Delta\tau \tag{20}$$

where C, the stress-optical coefficient, is a material property. In order to convert the physical stresses, τ_{12} and N_1, to the principal stresses, the stress tensor must be diagonalized with the result,

$$\tau_1 - \tau_2 = \sqrt{N_1^2 + 4\tau_{12}^2} \tag{21}$$

and

$$\tau_1 - \tau_3 = 1/2\,[N_1 + \sqrt{N_1^2 + 4\tau_{12}^2}] + N_2 \tag{22}$$

According to the Wagner model, N_2, the second normal stress difference, is identically zero, but a large body of data suggests that $N_2 \simeq -0.1N_1$ (Bird et al., 1987). We use this empiricism in an *ad hoc* fashion to evaluate the stress difference in Eq. 22. The stress differences in Eqs. 21 and 22 correspond to two independent birefringence components, Δn_{13}, the so-called "normal" birefringence, and Δn_{12}, the "transverse" birefringence. The Δn_{13} component will be "seen" by a beam traversing normal to the disk plane, whereas Δn_{12} will be "seen" by a beam traversing in the plane of the disk. Both components will vary spatially because of the temperature and shear-rate inhomogeneities in the cavity during the process cycle. Since the sought quantities are the apparent normal and transverse retardations, we need to average the residual stresses across the disk thickness in order to obtain the effective retardations "seen" by a beam passing through the disk. Thus, based on Eq. 20,

$$R_N \equiv 2H\,\langle \Delta n_{13} \rangle = 2C_M \int_0^H (\tau_1 - \tau_3)_R\, dz \tag{23}$$

and

$$R_T \equiv 2H\,\langle \Delta n_{12} \rangle = 2C_M \int_0^H (\tau_1 - \tau_2)_R\, dz \tag{24}$$

where $\langle\ \rangle$ implies spatial averaging, the subscript R denotes "residual" and C_M is the stress-optical coefficient of the polymer melt. The use of C_M to evaluate the frozen-in birefringence originating from flow stresses was proposed by Oda, White, and Clark (1978) and later confirmed by Isayev and Hieber (1980), Isayev (1983), and Greener and Pearson (1983). Generally, the normal retardation has a more direct impact on the performance of the optical disk, but since the beam passing through the substrate has a conical shape (see Figure 1), the transverse component of retardation should also have some effect on the recording performance. The significance of the transverse retardation in several optical storage systems was discussed by Marchant (1983, 1986a, 1986b), Yoshizawa and Matsubayashi (1986), Toda et al. (1987) and Iwasawa and Funakoshi (1988).

The numerical algorithm of the model delineated above is shown schematically in Figure 3. Computation of this algorithm was done in a batch mode on an IBM 3081 mainframe. Typically, the calculation is repeated at eight equidistant points along a radial trajectory, and at each radial position the stress analysis is conducted at 18 points across half the disk thickness. The average retardations for each position are evaluated based on Eqs. 23 and 24, thus obtaining radial profiles of R_N and R_T for a given set of material parameters and molding conditions. All the integrations in the model were performed numerically via the trapezoidal rule. The CPU time for a typical computation was approximately 30 min.

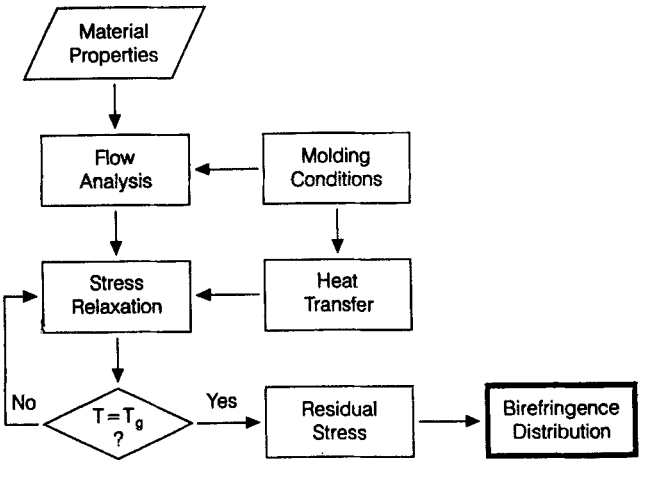

Figure 3. Numerical algorithm of the birefringence model.

Table 1. Material Parameters

Property*	Panlite AD5503** (PC)	Styron 685D*** (PS)
M_w, g/mol	3.36×10^4	3.12×10^5
PD	2.13	2.52
$K = A' \exp(B'/T)$		
A', Pa · s^n	1.44×10^{-7}	8.0
B', K	11,400	3,635
n	1.0	0.32
b	0.20	0.21
C_1	6.33	24.26
C_2, K	138	309.4
T_o, K	533	483
A	5.13×10^{-10}	6.131×10^{-11}
B, K	11,400	11,360
C_M, Pa^{-1}	3.5×10^{-9}	-4.5×10^{-9}
C_G, Pa^{-1}	9.2×10^{-11}	1.0×10^{-11}†
β, m^2/s	$\sim 1.0 \times 10^{-7}$†‡	$\sim 8.0 \times 10^{-8}$†
T_g, K	418	378

*See notation listing.
**This work except as noted.
***See Greener and Pearson (1983).
†van Krevelen and Hoftzyer (1976).
‡Tadmor, Z., and C. G. Gogos, *Principles of Polymer Processing*, Wiley, New York (1979).

Experimental

Material parameters

Many physical and rheological parameters must be input into the model in order to carry out a meaningful simulation. The material in most of the simulations was a typical resin used for molding optical disk substrates: Panlite AD5503 made by Teijin Chemical Industries of Japan. This material is a low-molecular-weight bisphenol-A polycarbonate (PC) designated for optical disk applications. (For the purposes of this simulation Panlite AD5503 is not inherently different from other optical disk grade PC's such as General Electric's Lexan OQ1010 or Mobay's Merlon CD2000.) This material is compared with a more conventional resin: Styron 685D made by Dow Chemical, which is a typical injection-grade atactic polystyrene. The key properties of these materials are listed in Table 1.

In addition to the properties given in Table 1, several sets of

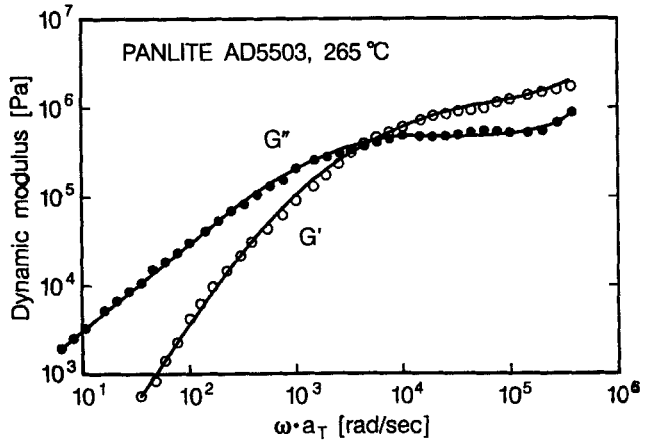

Figure 4. Dynamic moduli vs. reduced frequency for Panlite AD5503 at 265°C.
Points are experimental data and curves are analytically fitted functions.

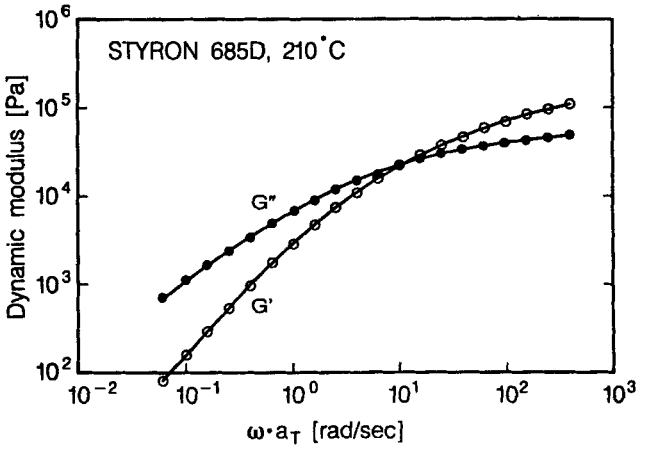

Figure 5. Dynamic moduli vs. reduced frequency for Styron 685D at 210°C.
Points are experimental data and curves are analytically fitted functions.

rheological parameters must be specified. The linear parameters of the Wagner model, μ_i and λ_i, were extracted from linear viscoelastic data for the molten polymers. The dynamic shear moduli for both materials are shown in Figures 4 and 5. The data are master curves obtained by shifting oscillatory data from several temperatures to a reference temperature T_0. All the oscillatory measurements were done on the Rheometrics System Four (Melts head) using a parallel disk geometry. The solid curves in Figures 4 and 5 are analytically fitted exponential functions (cf. Eq. 10) obtained by an optimization procedure described elsewhere (Greener and Connelly, 1986). The corresponding linear parameters for both materials are listed in Tables 2 and 3. The nonlinear parameter b (cf. Eq. 11) was obtained by fitting the shear viscosity function predicted by the Wagner model to experimental data. Viscosity data and fitted curves for both materials are shown in Figures 6 and 7 and the corresponding b's are listed in Table 1. The viscosity data were obtained by capillary viscometry using the Gottfert Rheograph 2001 system. It is seen that the PC resin is nearly Newtonian over a practical range of shear rates, whereas the PS resin is strongly shear thinning. The relaxation spectra in Tables 2 and 3 can be used to define an average relaxation time for the corresponding materials,

$$\lambda \equiv \frac{\sum_i \mu_i \lambda_i^3}{\sum_i \mu_i \lambda_i^2} \tag{25}$$

Table 2. Linear Viscoelastic Parameters of Panlite AD5503 (T_0 = 260°C)

i	λ_i (s)*	μ_i (Pa · s^{-1})
1	0.600E − 05	0.210E + 12
2	0.300E − 04	0.105E + 11
3	0.100E − 03	0.468E + 10
4	0.300E − 03	0.623E + 09
5	0.100E − 02	0.137E + 09
6	0.100E − 01	0.329E + 06
7	0.100E + 00	0.836E + 02

*$\lambda = 1.97 \times 10^{-3}$ s.

Table 3. Linear Viscoelastic Parameters of Styron 685D (T_0 = 210°C)

i	λ_i (s)*	μ_i (Pa · s^{-1})
1	0.100E − 02	0.906E + 08
2	0.300E − 02	0.674E + 07
3	0.100E − 01	0.354E − 07
4	0.300E − 01	0.894E + 06
5	0.100E + 00	0.171E + 06
6	0.300E + 00	0.275E + 05
7	0.100E + 01	0.283E + 04
8	0.300E + 01	0.187E + 03
9	0.100E + 02	0.125E + 02
10	0.300E + 02	0.659

*λ = 3.3 s.

The values of λ given in Tables 2 and 3 indicate that PS is considerably more elastic than PC. (This comparison is based on approximately the same temperature interval above T_g and not the same temperature.)

Injection molding and birefringence measurements

Several molding runs were conducted on a Meiki M-70A-D-DM injection-molding machine to produce 13-cm (dia.) polycarbonate substrates. The molding resin in all the runs was Panlite AD5503 (see Table 1) and the pertinent molding conditions and cavity dimensions are listed in Table 4. The only parameter varied in this experiment was the melt temperature. In Table 4 we list the set temperatures for the four zones in the barrel of the injection-molding machine, but only the temperature in the front zone is generally considered representative of the actual melt temperature. As is usually the case in injection-molding experiments, the exact melt temperature could not be determined independently and some uncertainty in the value of T_{melt} is expected. Likewise, the fill times in Table 4 were estimated from hydraulic pressure traces and are also not exact (cf. Greener and Pearson, 1983).

The normal retardation profiles in the molded substrates were measured following a standard procedure, and the transverse retardation was obtained from measurements in oblique incidence based on a procedure developed by Stein (1957). Both measurements were conducted with an optical train comprising a HeNe laser, crossed polars, and a Soleil-Babinet compensator.

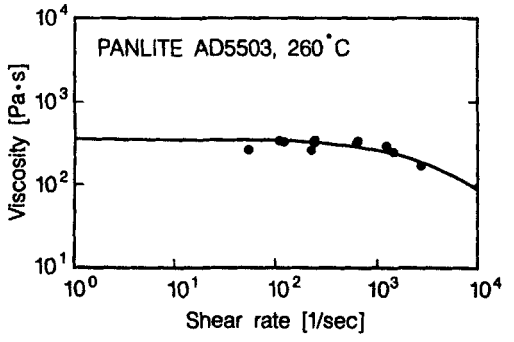

Figure 6. Viscosity vs shear rate for Panlite AD5503 at 260°C.
Points are experimental data and curve is fitted by the Wagner model.

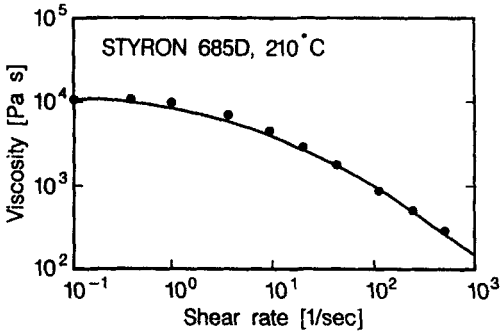

Figure 7. Viscosity vs shear rate for Styron 685D at 210°C.
Points are experimental data and curve is fitted by the Wagner model.

A detailed description of the procedures for measuring birefringence is given elsewhere (Machell et al., 1988).

Results and Discussion

Experimental retardation profiles for substrates molded under conditions listed in Table 4 are shown in Figures 8 and 9 together with predictions based on the front-zone temperature. Overall, the trends in R_N (Figure 8) are well reproduced by the model. In line with observation, the model shows that R_N is a monotone decreasing function of radial position and is strongly dependent on melt temperature. Similar data have been recently reported by Takeshima and Funakoshi (1986), also demonstrating the strong effect of melt temperature on normal retardation. The small discrepancy between the data and the predictions can be attributed mainly to the uncertainty in T_{melt} and the inexact treatment of the heat transfer during the filling stage. In most runs an error of ~10°C can account for the difference between the experimental data and the predicted curves. Packing and mold displacement which are not considered in the present analysis can also explain some of the disparity between the data and the analytical results.

The negative values of R_N in the data for Run No. 1 cannot be accounted for by the model as it cannot predict a sign reversal in the R_N profile. This change in sign may be caused by a packing effect (Greener, 1986). Generally, the effect of packing on birefringence is not straightforward since it involves a large increase in hydrostatic pressure, which in itself cannot induce anisotropic (orienting) deformation in the melt. However, if packing induces mold displacement (mold opening), some anisotropic

Table 4. Molding Conditions and Cavity Geometry

	Run 1	Run 2	Run 3	Run 4
T_{mold}, °C	100	100	100	100
t_{fill}, s	0.5	0.5	0.5	0.5
Packing Pres., MPa	5.6	5.6	5.6	5.6
Barrel Temp., °C				
nozzle	285	280	275	270
front	335	315	295	275
center	320	300	280	260
rear	300	280	260	240
Cavity Dimensions, cm	R_g = 1.5 R_o = 6.5 H = 0.06			

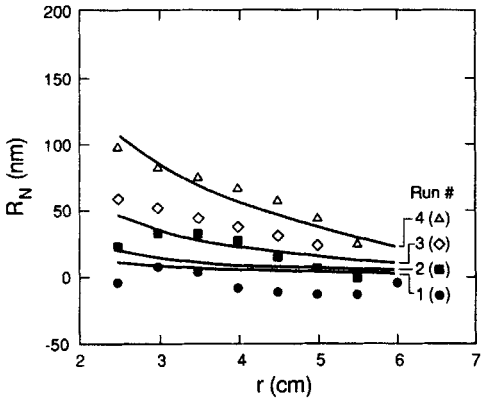

Figure 8. Radial profiles of normal retardation for runs 1 (●), 2 (■), 3 (+), and 4 (△).

See Table 4. Curves are model predictions based on front-zone temperature.

deformation may occur, leading to a drop in R_N and ultimately a sign reversal if the value of R_N is sufficiently low. Generally, we expect the effect of packing to be more pronounced at high melt temperatures and high packing pressures, especially when operating under low ("starved") clamping conditions (Greener, 1987).

In clear departure from the results in Figure 8, the observed transverse retardation (Figure 9) appears to be independent of radial position and melt temperature and is substantially higher than the values predicted by the model. This disparity implies that the origin of the transverse retardation is different from that of the normal retardation and thus cannot be properly treated by the present model. It was noted earlier that flow stress, on which the present model is based, is only one source of residual orientation in molded plastic articles. Another known mechanism for residual birefringence is cooling stress. This stress originates from the rapid and inhomogeneous cooling of the melt when it comes in contact with the cold walls of the mold and is known to induce distinct birefringence patterns in molded articles (cf. Isayev and Crouthamel, 1984; Greener and Pearson, 1983). (The injection-molding cycle can be viewed as a quenching process whereby a finite volume of a hot melt is rapidly cooled to below its glass-transition temperature.) Although several successful models for the cooling stress problem in freely quenched bodies have been developed over the years (Aggarwala and Saibel, 1961; Lee et al., 1965), extension of these models to the injection-molding problem is not trivial because of the constraints imposed on the material by the rigid confines of the cavity. One attempt to calculate cooling stresses in molded parts was made by Rigdahl (1976) using finite-element techniques, but the problem generally defies a simplified analysis. Without an exact solution of the problem, it is possible to use the theory of Aggarwala and Saibel (1961; see also Struik, 1978) to scale the residual cooling stresses in a molded slab by

$$\langle \tau_p \rangle \propto \frac{E\,\alpha(T_g - T_{\text{mold}})}{(1-\nu)} \tag{26}$$

where $\langle \tau_p \rangle$ is a stress operative in the plane of the slab (plane stress) averaged across the gap, α is the thermal expansion coefficient of the polymer, E is its Young's modulus, and ν is its Poisson's ratio. It follows then that the average transverse retardation can be scaled as

$$R_T \propto \frac{C_G E\,\alpha(T_g - T_{\text{mold}})}{(1-\nu)} \tag{27}$$

where C_G is the stress-optical coefficient of the glassy polymer. The rationale for using this property, rather than C_M, for example, was put forth in several recent studies (Isayev and Crouthamel, 1984; Greener and Kenyon, 1981; Wust and Bogue, 1983; Lee et al., 1986) and it derives from the fact that the freezing-in process for the cooling stress effect occurs in the glass-transition range. Inspection of Eq. 27 reveals that, to first order, R_T should be independent of radial position and melt temperature as indicated by the data in Figure 9, but it should increase linearly with C_G and $\Delta T_g \equiv T_g - T_{\text{mold}}$. Some evidence for the presence of residual cooling stresses in molded PC substrates is provided by Brekner (1988). Based on the above, PC should be at a distinct disadvantage in its propensity to induce high R_T since it has a relatively high C_G (cf. Table 1, and van Krevelen and Hoftyzer, 1976) and its ΔT_g is also likely to be high because of its high T_g.

Having demonstrated its ability to predict the normal retardation quantitatively, the model will now be used to illustrate the effects of three process parameters—melt temperature, mold temperature, and fill time (injection speed)—on R_N in disks molded with Panlite AD5503. The geometry in all cases is as specified in Table 4 and the nominal molding conditions are: $T_{\text{melt}} = 568$ K, $T_{\text{mold}} = 363$ K, and $t_{\text{fill}} = 0.5$ s. Unless otherwise noted, these values are implied throughout the simulation. Figure 10 illustrates again the dominant effect of T_{melt} on R_N. The effect of temperature can be attributed to two independent factors. First, the melt temperature controls the level of stress during the filling stage and at the instant of fill (initial stress) and, second, it has a strong effect on the rate of stress relaxation during the post-filling stage. At higher temperatures the initial stress is lower and the relaxation rate is faster, and hence the "frozen-in" birefringence is substantially reduced. The effect of mold temperature, Figure 11, is less pronounced, but here too an increace in T_{mold} leads to a drop in R_N. The increase in retardation at lower T_{mold} is due to faster cooling near the cavity walls (i.e., thicker skin) and, correspondingly, slower relaxation. The effect of T_{mold} on R_T, according to Eq. 27, is likely to be more

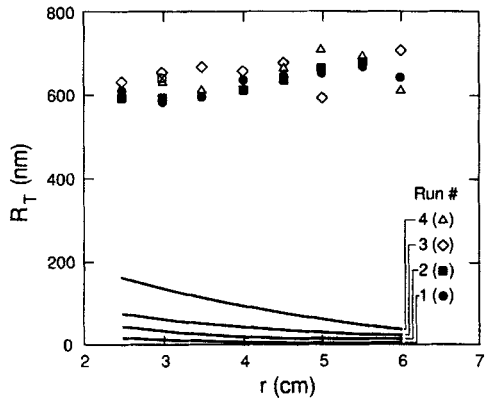

Figure 9. Radial profiles of transverse retardation for runs 1 (●), 2 (■), 3 (+), and 4 (△).

See Table 4. Curves are model predictions based on front-zone temperature.

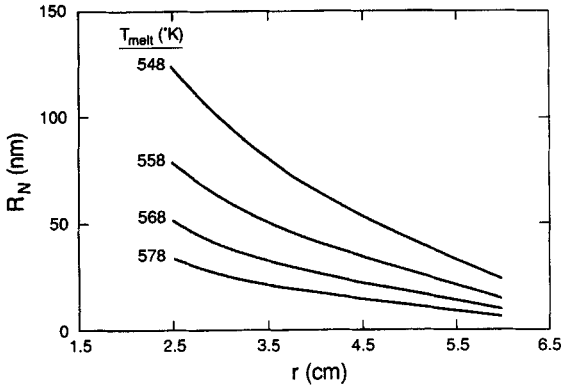

Figure 10. Model calculations of the effect of melt temperature on the normal retardation in a 130-mm disk substrate.

T_{mold} = 363 K; t_{fill} = 0.5 s. Material: Panlite AD5503.

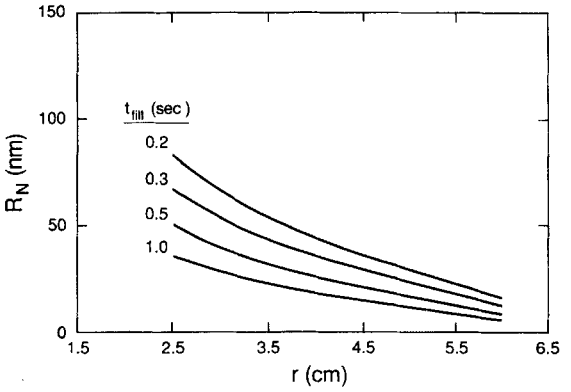

Figure 12. Model calculations of the effect of mold fill time on the normal retardation in a 130-mm disk substrate.

T_{melt} = 568 K; T_{mold} = 363 K. Material: Panlite AD5503.

pronounced than its effect on R_N; R_T is expected to decrease as T_{mold} approaches T_g.

The effect of fill time is shown in Figure 12. Here, an increase in fill time (decrease in flow rate) leads to a drop in retardation. This result is plausible but it should be taken with some caution. The approximate heat transfer analysis for the filling stage used in this study may not be valid at extreme fill times. For long fill times cooling may dominate the filling process, thus increasing the initial stress. Conversely, for short times (high shear rates), viscous heating effects may cause a significant rise in temperature and a corresponding drop in flow stress. This may moderate or even reverse the trend depicted in Figure 12.

Finally, we illustrate how the physical and rheological differences between the materials listed in Table 1 impact the normal retardation profile in the molded disk. When molded under the nominal conditions, PS is expected to generate considerably higher retardation than PC (Figure 13), even though the calculated pressure drop for PS, based on Eq. 8, is markedly lower (3.81 and 5.74 MPa for PS and PC, respectively). The differences in R_N can be ascribed partly to the higher stress-optical coefficient of PS but mainly to its more elastic character (longer relaxation time, cf. Tables 2 and 3). The latter is clearly illustrated in Figure 14 where residual stress profiles for both materials are compared at a specified radial position. In both cases, but especially for the PC disk, the skin layer dominates the level of residual stress near the surfaces. For the PC disk, however, the stresses fall off precipitously at the skin/core interface (position of maximum stress) and essentially vanish a small distance away from the skin. [Qualitatively similar profiles were observed by Takeshima and Funakoshi (1986) using laser Raman spectroscopy.] The skin is thinner in the case of PS owing to its lower Tg, but the residual stresses decay more gradually with z due to its longer relaxation time which may weigh more heavily on the gapwise-averaged retardation. The presence of an "outer" skin, generally associated with the fountain flow effect (Kamal et al., 1988; Vlachopoulus et al., 1988), is not considered in the present analysis. It is conceivable that this "outer" skin could contribute to the retardation level in the disk, but since it is usually confined to a very thin layer off the part walls, its overall effect on the gapwise-averaged birefringence is expected to be small.

Summary and Conclusions

An analytical model has been constructed to predict the flow-induced birefringence in an injection-molded disk with direct

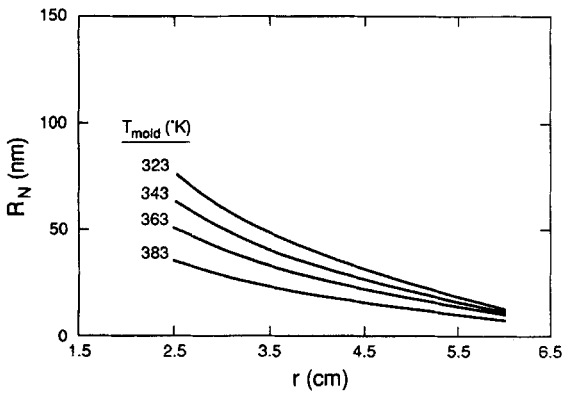

Figure 11. Model calculations of the effect of mold temperature on the normal retardation in a 130-mm disk substrate.

T_{melt} = 568 K; t_{fill} = 0.5 s. Material: Panlite AD5503.

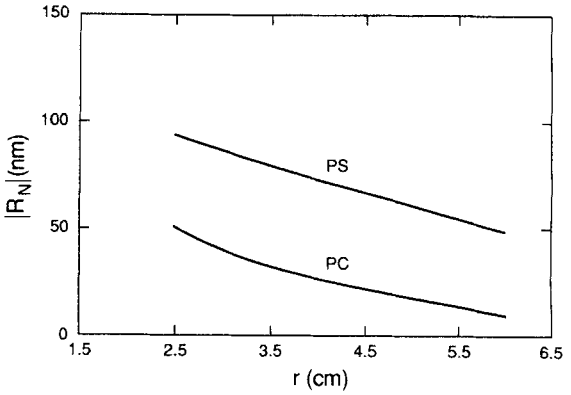

Figure 13. Model calculations of the effect of material on the normal retardation in a 130-mm disk: Styron 685D (PS) vs. Panlite AD5503 (PC).

T_{melt} = 568 K; T_{mold} = 363 K; t_{fill} = 0.5 s.

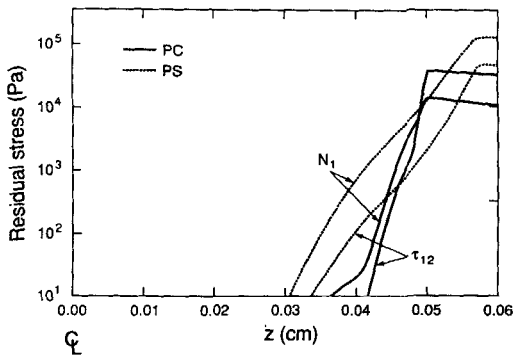

Figure 14. Model calculations of residual stress profiles in the a 130-mm disk at r = 3.5 cm: Styron 685D (PS) vs. Panlite AD5503 (PC).
T_{melt} = 568 K; T_{mold} = 363 K; t_{fill} = 0.5 s.

application to optical disk substrates. The model incorporates simplified analyses for the stress buildup during the filling stage, the heat transfer during the cooling stage, and the stress relaxation following the cessation of flow in the center-gated disk cavity at the end of the filling stage of the injection-molding cycle. The flow analysis, based on the purely viscous power-law approximation, is used to evaluate the flow kinematics in the cavity at the end of the filling stage. Nonisothermal effects during flow are approximately accounted for through the incorporation of a skin layer. Based on the known kinematics, the evolution of stress in the cavity after the cessation of flow is calculated with the nonlinear viscoelastic model of Wagner. The changes in temperature during the stress relaxation process are coupled with the relaxation analysis using the general approach of Matsui and Bogue (1977). The residual stresses are finally converted to birefringence via the stress-optical law and radial profiles of normal and transverse retardation are obtained by averaging the corresponding components of birefringence along the gapwise (thickness) direction.

The predictions of the normal retardation are generally in good agreement with experimental data; the general shape of the retardation profile, the dominant role of melt temperature, and the effects of mold temperature and fill time (injection speed) are properly predicted by the model. The analysis also indicates that the stress-optical coefficient and the relaxation time of the polymer are two key material parameters; a reduction in both should drastically lower the normal retardation in the disk. The transverse retardation, by contrast, is improperly described by the model. The discrepancy, both qualitative and quantitative, is attributed to the fact that the transverse retardation is induced, most likely, by residual cooling stresses, rather than flow stresses on which the present model is based. This implies that the transverse retardation can be minimized by operating at high mold temperatures and by using materials with a low stress-optical coefficient in the glassy state (cf. Eq. 27). Overall, the model should prove helpful in devising rational strategies for birefringence minimization in injection molding and in evaluating new polymers for use in optical disk substrates.

Acknowledgements

We wish to thank Mr. R. W. Connelly for the dynamic mechanical data and Ms. J. S. Machell for the measurement of the stress-optical coefficients of polycarbonate and polystyrene. Thanks are also due Dr. G. H. Pearson for reviewing the manuscript and providing helpful comments.

Notation

a = function defined in Eq. 1
a_T = time-temperature shift factor
A, B = parameters in Arrhenius equation (Eq. 18)
b = parameter in the Wagner model (Eq. 11)
C_1, C_2 = parameters in the WLF equation (Eq. 17)
C^{-1} = the Finger strain tensor
C_G, C_M = stress-optical coefficients in the glassy and molten states
h = the damping function (Eq. 11)
E = Young's modulus
$g_i = -\mu_i \lambda_i$
G = the shear relaxation modulus
H = half the disk thickness
$H_{eff} = H - \delta$
K = consistency index in the power-law model
M_W = weight-average molecular weight
n = power-law index
N_1 = first normal stress difference
N_2 = second normal stress difference
PD = polydispersity
$q = -1/n + 1$
Q = volumetric flow rate
r = radial coordinate (flow direction, "1")
R_g = radial position of gate
R_O = radius of substrate
R_N = normal retardation
R_T = transverse retardation
s = elapsed time
t = time
t_c = contact time
T = temperature
T_0 = reference temperature
T_g = glass-transition temperature
T_{melt} = melt temperature
T_{mold} = mold temperature
u_r, u_z, u_ϕ = velocity components
z = gapwise coordinate ("2")

Greek letters

α = thermal-expansion coefficient
β = thermal diffusivity
γ = shear strain
$\dot{\gamma}$ = rate of strain tensor
$\dot{\gamma}$ = shear rate
δ = skin layer thickness
Δn = birefringence
ΔP = pressure drop
$\Delta\tau$ = principal stress difference
λ = average relaxation time (Eq. 25)
λ_i = discrete relaxation time (Eq. 10)
μ = linear portion of the factorized memory function in Wagner's equation (Eq. 9)
μ_i = front factors in $\mu(t)$ (Eq. 10)
τ = deviatoric stress tensor
τ_{12} = shear stress
ϕ = "neutral" coordinate ("3")
I_c, II_c = first and second invariants of C^{-1}
$II_{\dot{\gamma}}$ = second invariant of $\dot{\gamma}$

Literature Cited

Aggarwala, B. D., and E. Saibel, "Tempering Stresses in an Infinite Glass Plate," *Phys. Chem. Glasses*, **2**, 137 (1961).
Ballman, R. L., and H. L. Toor, "Orientation in Injection Molding," *Mod. Plast.*, **38**, 113 (1960).
Bird, R. B., O. Hassager, and R. C. Armstrong, *Dynamics of Polymeric Liquids: 1. Fluid Mechanics*, 2nd ed., Wiley, New York (1987).

Bird, R. B., W. E. Stewart, and E. N. Lightfoot, *Transport Phenomena,* Wiley, New York (1960).
Brekner, M.-J., "Orientational and Stress Birefringence in Optical Disk Substrates," *Polym. Prep.*, **29,** 234 (1988).
Co, A., "Inelastic Flow from a Tube into a Radial Slit," *Ind. Eng. Chem. Fund.*, **20,** 340 (1981).
Dietz, W., J. L. White, and E. S. Clark, "Orientation Development and Relaxation in Injection Molding of Amorphous Polymers," *Polym. Eng. Sci.*, **18,** 273 (1978).
Ferry, J. D., *Viscoelastic Properties of Polymers,* 2nd ed., Ch. 11, Wiley, New York (1970).
Goyal, S. K., E. Chu, and M. R. Kamal, "Nonisothermal Radial Filling of Center-Gated Disc Cavities with Viscoelastic Polymer Melts," *J. Non-Newt. Fl. Mech.*, **28,** 373 (1988).
Greener, J., "General Consequences of the Packing Phase in Injection Molding," *Polym. Eng. Sci.*, **26,** 886 (1986).
Greener, J., "General Remarks on the Hybrid Molding Process," *ANTEC Proc.*, SPE, 238, Los Angeles (May, 1987).
Greener, J., and R. W. Connelly, "The Response of Viscoelastic Liquids to Complex Strain Histories: The Thixotropic Loop," *J. Rheol.*, **30,** 285 (1986).
Greener, J., and P. M. Kenyon, "Thermal Stresses in Amorphous Plastics," *J. Rheol.*, **297,** 99 (1981).
Greener, J., and G. H. Pearson, "Orientation Residual Stresses and Birefringence in Injection Molding," *J. Rheol.*, **27,** 115 (1983).
Isayev, A. I., "Orientation Development in the Injection Molding of Amorphous Polymers," *Polym. Eng. Sci.*, **23,** 271 (1983).
Isayev, A. I., and D. L. Crouthamel, "Residual Stress Development in the Injection Molding of Polymers," *Polym.-Plast. Technol. Eng.*, **22,** 177 (1984).
Isayev, A. I., and C. A. Hieber, "Toward a Viscoelastic Modelling of the Injection Molding Process," *Rheol. Acta,* **19,** 168 (1980).
Iwasawa, A., and N. Funakoshi, "Birefringence Analysis of Injection-Molded PC Substrates," *Polym. Prep.*, **29,** 237 (1988).
Janeschitz-Kriegl, H., "Injection Molding of Plastics: Some Ideas About the Relationship between Mould Filling and Birefringence," *Rheol. Acta,* **16,** 327 (1977).
Janeschitz-Kriegl, H., "Injection Molding of Plastics: II. Analytical Solution of Heat Transfer Problem," *Rheol. Acta.*, **18,** 693 (1979).
Kaempf, G., H. Loewer, and M. W. Witman, "Polymers as Substrates and Media for Data Storage," *Polym. Eng. Sci.*, **27,** 1421 (1987).
Kato, Y., S. Imai, M. Isobe, K. Manabe, and T. Nakarai, "Molding Compounds for Optical Disk Substrates," *SPIE,* **695,** 38 (1986).
Kamal, M. R., S. K. Goyal, and E. Chu, "Simulation of Injection Mold Filling of Viscoelastic Polymer with Fountain Flow," *AIChE J.*, **34,** 94 (1988).
Kirkland, C., "Super-Precision Disk Molding," *Plast. Tech.*, **19,** (1986).
Larson, R. G. and K. Monroe, "The BKZ as an Alternative to the Wagner Model for Fitting Shear and Elongational Flow Data of a LDPE Melt," *Rheol. Acta,* **23,** 10 (1984).
Lawrencena, B. R., and M. C. Williams, "Radial Flow of non-Newtonian Fluids Between Parallel Plates," *Trans. Soc. Rheol.*, **18,** 331 (1974).
Lee, S., J. de la Vega, and D. C. Bogue, "Residual Stresses and Birefringence in Large, Quenched Samples," *J. Appl. Polym. Sci.*, **31,** 2791 (1986).
Lee, E. H., T. G. Rogers, and T. C. Woo, "Residual Stresses in a Glass Plate Cooled Symmetrically from Both Surfaces," *J. Amer. Ceram. Soc.*, **48,** 480 (1965).
Machell, J. S., J. Greener, and B. A. Contestable, "The Optical Properties of Solvent Cast Polymer Films," to be submitted to *Macromolec.* (1988).
Marchant, A. B., "Cover Sheet Aberrations in Optical Recording," *SPIE Proc.*, **421,** 85 (1983).
Marchant, A. B., "Retardation Effects in Magneto-Optic Readout," SPIE Conf. on Mass Optical Data Storage II, San Diego (Aug., 1986a).
Marchant, A. B., "Index Variations in Cover Sheets," *Appl. Opt.*, **25,** 490 (1986b).
Matsui, M., and D. C. Bogue, "Studies in Non-isothermal Rheology," *Trans. Soc. Rheol.*, **21,** 133 (1977).
Menezes, E. V., "Some Relations and Tests on a Constitutive Equation with a Factorized Memory Function," *J. Non-Newt. Fl. Mech.*, **7,** 45 (1980).
Middleman, S., *Fundamentals of Polymer Processing,* Ch. 11, McGraw-Hill, New York (1976).
Oda, K., J. L. White, and E. S. Clark, "Influence of Melt Deformation History on Orientation in Vitrified Polymers," *Polym. Eng. Sci.*, **18,** 53 (1978).
Ojima, M., A. Saito, T. Kaku, M. Ito, Y. Tsunoda, S. Takayama, and Y. Sugita, "Compact Magnetooptical Disk for Coded Data Storage," *Appl. Opt.*, **25,** 483 (1986).
Richardson, S. M., "Injection Moulding of Thermoplastics: Freezing During Mould Filling," *Rheol. Acta,* **22,** 223 (1983).
Rigdahl, M., "Calculation of Residual Thermal Stresses in Injection Molded Amorphous Polymers by the Finite Element Method," *Int. J. Polym. Mat.*, **5,** 43 (1976).
Spencer, R. S., and G. D. Gilmore, "Some Flow Phenomena in the Injection Molding of Polystyrene," *J. Colloid Sci.*, **6,** 118 (1951).
Stein, R. S., "Measurement of Birefringence of Biaxially Oriented Films," *J. Polym. Sci.*, **24,** 383 (1957).
Struik, L. C. E., "Orientation Effects and Cooling Stresses in Amorphous Polymers," *Polym. Eng. Sci.*, **18,** 799 (1978).
Takeshima, M., and N. Funakoshi, "Molecular Orientation Distribution in Injection-Molded Polycarbonate Discs," *J. Appl. Polym. Sci.*, **32,** 3457 (1986).
Toda, T., K. Shigematsu, M. Yoshihiro, M. Ojima, and Y. Tsunoda, "Analysis of Signal to Noise Ratio in Magneto-Optical Disk Using a Polarization Simulator," *Optical Data Storage-Technical Digest,* **10,** 34 (1987).
van Krevelen, D. W., and P. J. Hoftyzer, *Properties of Polymers,* Elsevier, Amsterdam (1976).
Vlachopoulos, J., H. Mavrides, and A. N. Hrymak, "Rheological Problems in the Injection Molding of Polymers," *Proc. Int. Cong. Rheology,* **2,** 351, Sydney, Australia (1988).
Wagner, M. H., "Analysis of Stress-Growth Data for Simple Extension of a Low-Density Polyethylene Melt," *Rheol. Acta,* **15,** 133 (1976).
Wagner, M. H., "Zur Netzwerktheorie von Polymer Schmelzen," *Rheol. Acta,* **18,** 33 (1979).
Wagner, M. H., T. Raible, and J. Meissner, "Tensile Stress Overshoot in Uniaxial Extension of a LDPE Melt," *Rheol. Acta,* **18,** 427 (1979).
Wagner, M. H., and S. E. Stephenson, "The Irreversibility Assumption of Network Disentanglement in Flowing Polymer Melts and its Effects on Elastic Recoil Predictions," *J. Rheol.*, **23,** 489 (1979).
Wales, J. L. S., I. J. van Leeuwen, and R. Vander Vijgh, "Some Aspects of Orientation in Injection Molded Objects," *Polym. Eng. Sci.*, **12,** 358 (1972).
Wust, C. J., and D. C. Bogue, "Stress Optical Behavior in Polystyrene; Residual Stresses and Birefringence in Large, Quenched Samples," *J. Appl. Polym. Sci.*, **28,** 1931 (1983).
Yoshizawa, A., and N. Matsubayashi, "Analysis of Optical Anisotropy of PC Substrate for M-O Disc and Its Effect on CNR," *SPIE,* **695,** 91 (1986).

Manuscript received June 8, 1988, and revision received Oct. 17, 1988.